International Journal of Engineering

Journal Homepage: www.ije.ir

Sensorless Model Predictive Force Control with a Novel Weight Coefficients for 3-Phase 4-Switch Inverter Fed Linear Induction Motor Drives

S. Masomi Kazraji*, M. R. Feyzi, M. B. B. Sharifian, S. Tohidi

Faculty of Electrical and Computer Engineering University of Tabriz, Tabriz, Iran

P A P E R I N F O

Paper history:
Received 27 December 2017
Received in revised form 14 April 2018
Accepted 26 April 2018

Keywords:
Linear Induction Motor
Sensorless Model Predictive Force Control
4-switch Inverter
Weight Coefficient

A B S T R A C T

The sensorless model predictive force control (SMPFC) is a strong method for controlling the drives of three-phase 4(6)-switch inverter linear induction motors. This kind of inverter can be employed for the fault tolerant control in order to solve the problem of open/short circuit in the 6-switch inverters (B6). This paper propose a method for the SMPFC of a linear induction motor (LIM) fed by a 4-switch inverter fed along with DC-link voltage offset reduction. Simulations have been performed on several different LIMs in MATLAB software to determine the weight coefficients of stator flux and reduction of the capacitor voltage offset. Then, a relationship has been proposed for determining the weight coefficients in the cost function of the SMPFC. By using weight coefficients in the cost function, the B4 inverter voltage vectors are obtained for exact prediction. The balance of currents is improved by determining the appropriate value for the weight coefficient of the capacitor voltage offset reduction. Simulation results are provided for validation of the suggested control method.

***doi**: 10.5829/ije.2018.31.09c.09*

NOMENCLATURE

R_s, R_r	Primary and Secondary resistances	l_{ls}, l_{lr}	Primary and Secondary leakage inductances
$\lambda_{ds}, \lambda_{dr}$	Primary and Secondary fluxes of d axe	l_m	Magnetizing inductance
$\lambda_{qs}, \lambda_{qr}$	Primary and Secondary fluxes of q axe	L_p	Primary length
τ , T_s	Pole pitch, sampling time	p	Pole number
k_λ	weight coefficient of the stator flux	i_{ds}, i_{dr}	Primary and Secondary currents of d axes
U_{dc1},U_{dc2}	Capacitor voltages of the upper and lower DC-link	i_{qs}, i_{qr}	Primary and Secondary currents of q axe
g	Cost function	$v_l, \hat{v}_l$	Real and estimated linear speed
l_s, l_r	Primary and Secondary self-inductances	$u_{ds}, u_{dr}, u_{qs}, u_{qr}$	Primary and Secondary voltages of dq axes
U_{dc1}, U_{dc2}	capacitor voltages of DC-link.	j	index of the stator voltage vector
N_s	number of switching	T_{dead}	dead time

1. INTRODUCTION

Linear induction motors (LIMs) have several advantages such as need for no interface mechanical tools, low mechanical loss, high starting force, and a simple and strong structure. Such motors are used in automation and industrial applications, e.g. transportation, conveyor drives, electromagnetic launchers, and transfer of the containers in container terminals. Among different LIMs, single-side LIMs have received more attention due to their simpler structure and higher stability [1-3].

LIMs have complicated mathematical model. The non-linear and multi-variable structure of these motors makes simple control methods unable to control their

*Corresponding Author Email: *masoumikazraji@tabrizu.ac.ir* (S. Masoumi Kazraji)

Please cite this article as: S. Masomi Kazraji, M. R. Feyzi, M. B. B. Sharifian, S. Tohidi, Sensorless Model Predictive Force Control with a Novel Weight Coefficients for 3-Phase 4-Switch Inverter Fed Linear Induction Motor Drives, International Journal of Engineering (IJE), IJE TRANSACTIONS C: Aspects Vol. 31, No. 9, (September 2018) 1536-1545

electromagnetic characteristics. In addition, existence of the traversal edge and longitudinal end effects creates difficulties in the modeling and controlling of such motors [4].

In recent years, inverters with 6 switches (B6) have been employed for applications such as motor drives. However, in some applications, further cost reduction for the structure of inverters has been proposed. In [1], a three-phase inverter with 4 switches (Figure 1) is suggested to minimize the costs of inverter, named as three-phase 4-switch inverter (B4). Also this inverter solves the problem of open circuit/short circuit in B6 inverters. The idea of applying 4-switch inverters for fault-tolerant control is valuable in some applications, including tensile systems [5-7]. 4-switch inverters have a number of flaws in comparison with B6 inverters. Their voltage utilization coefficient is half that of B6 inverters. Moreover, the capacitor voltage swings, interrupting the balance of motor currents. The fluctuations of capacitor increase the force ripple and reduce the inverter frequency.

Several methods have been proposed to reduce the effect of capacitor swings. A comparative space vector modulation method is introduced to compensate for the DC-link voltage ripple [8]. In [9], the capacitor voltage offset is neutralized by applying certain switching modes. Despite achieving a balance between the phase currents, this paper does not consider the flux and stator force. A closed-loop vector control method with a 4-switch inverter is examined [10]. In this method, speed loop is controlled with fuzzy logic controller. Also in [11], direct torque control is employed to control the flux and torque of induction motor with a 4-switch inverter. In this paper, the capacitors voltage is assumed to be constant. In fact, the one-phase current passes through DC-link voltage sources, resulting in fluctuations in the capacitor voltages.

Among the control methods, field-oriented control and direct force control (DFC) have received considerable attention for controlling LIM [12]. With development of fast microprocessors, the use of model predictive control (MPC) in the power electronic drives has become widespread [13, 14].

In predictive torque control, the complete model and the drives fed with the inverter are considered. A cost function is defined to reduce the torque and flux error in order to evaluate the effect of voltage vectors [15, 16].

The present paper is organized as follows: In section 2, dynamic models of LIM and three-phase 4-switch inverters are explained. In section 3, the predictive control method is expressed by removing the capacitor voltage. In sections 4 and 5, the weighting coefficients in the cost function and the results of simulation and real-time hardware-in-the-loop results are respectively analyzed. Finally, in section 6, the conclusions from the proposed control algorithm are provided.

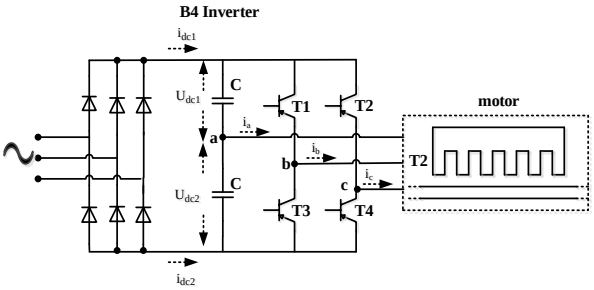

Figure 1. Circuit diagram of the induction motor fed by B4 inverter

2. MATHEMATICAL MODEL of LIM AND 4-SWITCH INVERTER

2. 1. Mathematical Model of LIM The relationships of the primary voltage in the synchronous dq reference frame are as follows [2, 13]:

$$u_{ds} = R_s i_{ds} + R_r f(Q)(i_{ds} + i_{dr}) + \frac{d}{dt}\psi_{ds} \quad (1)$$

$$u_{qs} = R_s i_{qs} + \frac{d}{dt}\psi_{qs} \quad (2)$$

The relationships of the secondary voltage are:

$$u_{dr} = R_r i_{dr} + \frac{\pi}{\tau}\upsilon_r \psi_{qr} + R_r f(Q)(i_{ds} + i_{dr}) + \frac{d}{dt}\psi_{dr} \quad (3)$$

$$u_{qr} = R_r i_{qr} - \frac{\pi}{\tau}\upsilon_r \psi_{dr} + \frac{d}{dt}\psi_{qr} \quad (4)$$

$$f(Q) = \frac{1 - e^{-Q}}{Q} \quad (5)$$

$$Q = \frac{L_p / v_r}{(L_m + L_r)/R_r} \quad (6)$$

The electromagnetic force of the LIM is calculated as:

$$F_e = \frac{3}{2}\frac{\pi}{\tau}\frac{P}{2}(\lambda_{ds} i_{qs} + \lambda_{qs} i_{ds}) \quad (7)$$

The primary and secondary currents dq for LIM are calculated by Equations (1)-(6):

$$i_{ds} = \frac{L_r - L_m f(Q)\lambda_{ds} - L_m(1 - f(Q))\lambda_{dr}}{(L_s - L_m f(Q))(L_r - L_m f(Q)) - L^2{}_m(1 - f(Q))^2} \quad (8)$$

$$i_{qs} = \frac{L_r \lambda_{qs} - L_m \lambda_{qr}}{L_s L_r - L^2{}_m} \quad (9)$$

$$i_{dr} = \frac{(L_s - L_m f(Q))\lambda_{dr} - L_m(1 - f(Q))\lambda_{ds}}{(L_s - L_m f(Q))(L_r - L_m f(Q)) - L^2{}_m(1 - f(Q))^2} \quad (10)$$

$$i_{qr} = \frac{L_s \lambda_{qr} - L_m \lambda_{qs}}{L_s L_r - L^2{}_m} \tag{11}$$

f(Q) is utilized to take the end effect of the LIM into account in Equation (5).

2. 2. Mathematical Model of the 4-Switch Inverter

B4 is a two-base inverter, as demonstrated in Figure 1. In order to have a better analysis, the inverter is implemented with ideal switches (T1-T4) [11]. This means that the basic switching modes b and c can be shown as binary variables Sb and Sc. In order to avoid the short circuit of DC-link, the switches are prevented from being on simultaneously. Therefore, the binary number "1" indicates the closed mode of upper switch and the binary number "0" denotes the closed mode of the lower switch. Assuming that the 3-phase voltages are symmetrical, the phase-to-neutral voltages U_{aN}, U_{bN} and U_{cN} are defined as:

$$\begin{aligned} U_{aN} &= \frac{U_{dc1}}{3}(-S_b - S_c) + \frac{U_{dc2}}{3}(2 - S_b - S_c) \\ U_{bN} &= \frac{U_{dc1}}{3}(2 \cdot S_b - S_c) + \frac{U_{dc2}}{3}(2S_b - S_c - 1) \\ U_{cN} &= \frac{U_{dc1}}{3}(2S_c - S_b) + \frac{U_{dc2}}{3}(2S_c - S_b - 1) \end{aligned} \tag{12}$$

By taking all the possible cases of Sb and Sc into account, the phase-to-neutral voltage values are provided in Table 1. If the upper and lower capacitor values are enough to maintain the capacitor voltage constant in $U_{dc}/2$, 4 voltage vectors with 4 possible combinations are produced (Figure 2a). The states of vectors in Figures 2(b) and 2(c) are shown in $U_{dc1}<U_{dc2}$ and $U_{dc1}>U_{dc2}$ modes. The position of the vectors is calculated and illustrated in Figure 2.

3. MPFC for LIM DRIVE with 4-SWITCH INVERTER

In the proposed method, the flux and force controllers are PFC. Based on the standard PFC method, a 2-mode algorithm is done: prediction of flux and force, and optimization of the cost function [18- 21].

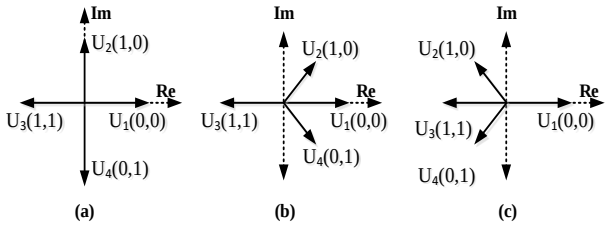

Figure 2. Voltage vectors of the 4-switch inverter in the case of: (a) $U_{dc1}=U_{dc2}$, (B) $U_{dc1}<U_{dc2}$, (C) $U_{dc1}>U_{dc2}$

The structure of LIM drive fed by the B4 inverter using the PFC method is depicted in Figure 3.

3. 1. Prediction of the Flux and Force The accurate estimation of flux and force is necessary for the accurate performance of MPFC. In this paper, a Luenberger observer is adapted in the fast speed range for high precision. With introduction of the stator current error feedback, the precision of estimation and observer became more resistant against the change of motor parameters.

The LIM model are are state as follows:

$$\frac{d}{dt}\begin{bmatrix} i_{ds} \\ i_{qs} \\ \lambda_{dr} \\ \lambda_{qr} \end{bmatrix} = \begin{bmatrix} -\frac{R_r + R_s}{L_{ls}} & 0 & \frac{R_r}{ML_{ls}} & \frac{p}{2}\frac{\pi}{\tau}\frac{v_l}{Lls} \\ 0 & -\frac{R_r + R_s}{L_{ls}} & -\frac{p}{2}\frac{\pi}{\tau}\frac{v_l}{Lls} & \frac{R_r}{ML_{ls}} \\ R_r & 0 & -\frac{R_r + R_{sh}}{M} & -\frac{p}{2}\frac{\pi}{\tau}v_l \\ 0 & R_r & \frac{p}{2}\frac{\pi}{\tau}v_l & -\frac{R_r + R_{sh}}{M} \end{bmatrix} \times \begin{bmatrix} i_{ds} \\ i_{qs} \\ \lambda_{dr} \\ \lambda_{qr} \end{bmatrix} + \begin{bmatrix} \frac{1}{Lls} & 0 \\ 0 & \frac{1}{Lls} \\ 0 & 0 \\ 0 & 0 \end{bmatrix} \begin{bmatrix} u_{ds} \\ u_{qs} \end{bmatrix} \tag{13}$$

where, $M = L_m(1 - f(Q))$, $R_{sh} = R_r f(Q)$.

The mathematical model of the observer by using Equation (1) for LIM, is as follows:

$$\frac{d\hat{x}}{dt} = A\hat{x} + Bu + G(i_s - \hat{i}_s) \tag{14}$$

where, $\hat{x} = \begin{bmatrix} \hat{i}_s & \hat{\lambda}_s \end{bmatrix}^T$ are the variables of estimation.

In the classic observer for the drives of LIMs, the poles of observer are designed proportional to the poles of the LIM [21], which creates a large imaginary part at high speeds. In order to solve this issue, movement of the real part of observer poles to the left in the complex design in comparison with the poles of LIM has been proposed, while the imaginary part of the observer poles does not change [22-24]. This method of movement is easy to implement and improves the convergence and stability of observer, especially at high speeds.

The flux and current of stator at k+1and k+2 moments are calculated from the Equation (13) and its adjustment were calculated by Equation (14). With the current at k+1 and k+2 moments, the electromagnetic force of Equation (7) is calculated as follows:

$$\begin{aligned} &F_e(k+1) = F_e(k) \\ &+ \frac{3}{2}\frac{\pi}{\tau}\frac{P}{2}\left(\lambda_{ds}(k+1)i_{qs}(k+1) - \lambda_{qs}(k+1)i_{ds}(k+1)\right) \\ &F_e(k+2) = F_e(k+1) \\ &+ \frac{3}{2}\frac{\pi}{\tau}\frac{P}{2}\left(\lambda_{ds}(k+2)i_{qs}(k+2) - \lambda_{qs}(k+2)i_{ds}(k+2)\right) \end{aligned} \tag{15}$$

TABLE 1. Switching functions and output voltages of B4 inverter

States		Switch On		Output Voltage		
Sb	Sc			U_{aN}	U_{bN}	U_{cN}
0	0	T_2	T_4	2 .U_{dc2}/3	-U_{dc2}/3	-U_{dc2}/3
0	1	T_2	T_3	(U_{dc2}-U_{dc1})/3	-(2U_{dc2}+U_{dc1})/3	2(U_{dc2}+U_{dc1})/3
1	0	T_1	T_4	(U_{dc2}-U_{dc1})/3	(2U_{dc2}+U_{dc1})/3	(2U_{dc2}+U_{dc1})/3
1	1	T_1	T_3	2 .U_{dc1}/3	U_{dc1}/3	U_{dc1}/3

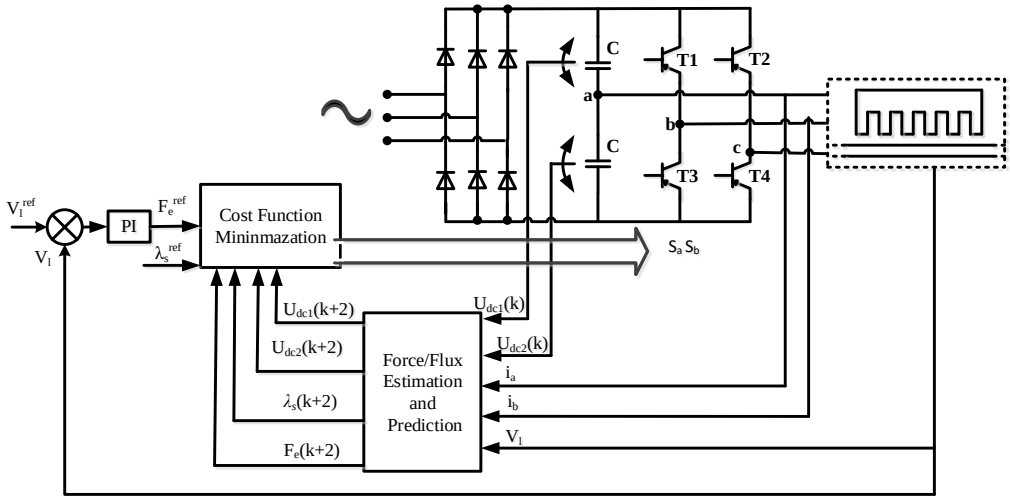

Figure 3. Structure of the B4 inverter-fed linear induction motor with the PFC method.

3. 2. The Cost Function As mentioned before, the stator flux and force is predicted as primary states using the predictive model with the $i_s(k)$ and $\lambda_s(k)$ variables at the moment of $k+1$ [25]. The aim is to make the stator flux and force follow their references. In other words, the error between the estimated flux and force, and their reference values should be minimized. This yields a cost function as follows:

$$g_j = \left|F_e^{ref} - \hat{F}_e(k+1)_j\right| + k_\lambda \left\|\lambda_s^{ref}\right| - \left|\hat{\lambda}_s(k+1)_j\right\| \qquad (16)$$
$$j \in \{1,2,3,4\}$$

We knew that there is a single-stage delay in the digital implementation. In other words, the chosen voltage vector at moment k would not be applied at moment k+1 [25-28]. In order to remove this delay, in Equation (16) the amount at k+2 moment is assumed to be proportional to k+1 moment; therefore, the cost function is rewritten as follows:

$$g_j = \left|F_e^{ref} - \hat{F}_e(k+2)_j\right| + k_\lambda \left\|\lambda_s^{ref}\right| - \left|\hat{\lambda}_s(k+2)_j\right\| \qquad (17)$$
$$j \in \{1,2,3,4\}$$

3. 3. Reduction of Voltage DC-Link offset The improper angle of the current of phase "a" or imbalance of the current in two capacitors results in deviation of the voltage [10]. According to Figure 2, the offset of capacitor voltage is related to the gain increase of the inverter and the reliable performance of 4-switch inverter. Hence, it is necessary to remove the offset of capacitor voltages. Consider the $U_4(1,0)$ switching mode shown in Figure 4. Two current loops are created. Then, i_{dc1} and i_{dc2} are calculated. By the same method, the DC-link current of the other three vectors is calculated. The currents of the DC-link is expressed as follows:

$$i_{dc1} = i_b.S_b + i_c.S_c$$
$$i_{dc2} = i_b.(1-S_b) + i_c.(1-S_c) \qquad (18)$$

In the above equations, i_{dc1} and i_{dc2} are the currents of the upper and lower DC-links respectively, and i_b and i_c are the currents of phases. By knowing the capacitor currents (18), the voltage of the capacitor is calculated as follows:

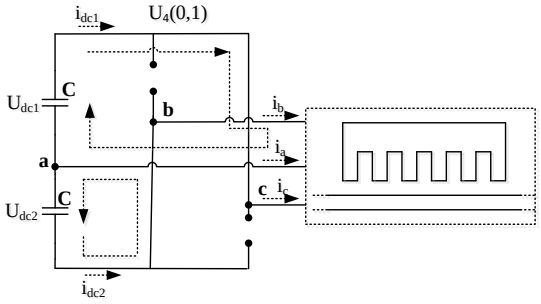

Figure 4. Current paths in the switching mode U_4

$$\hat{U}_{dc1} = U_{dc1} + (1/C)\int_{t_0}^{t}(-i_{dc1})dt$$
$$\hat{U}_{dc2} = U_{dc2} + (1/C)\int_{t_0}^{t} i_{dc2}dt \quad (19)$$

where, C is the capacity of DC-link capacitors.

By employing the Euler formula for discretization (18), the capacitor currents at the k sampling time are calculated as follows:

$$i_{dc1}(k) = i_b(k).S_b + i_c(k).S_c$$
$$i_{dc2}(k) = i_b(k).(1-S_b) + i_c(k).(1-S_c) \quad (20)$$

Moreover, using the Euler formula for discretization (19), $\hat{V}_{dc1}(k+1)$ and $\hat{V}_{dc2}(k+1)$ at the k+1 time are calculated as follows:

$$\hat{U}_{dc1}(k+1) = \hat{U}_{dc1}(k) - (1/C).i_{dc1}(k).T_s$$
$$\hat{U}_{dc2}(k+1) = \hat{U}_{dc2}(k) + (1/C).i_{dc2}(k).T_s \quad (21)$$

$\hat{U}_{dc1}(k+1)$ and $\hat{U}_{dc2}(k+1)$ are calculated using a similar method.

In order to reduce the capacitor voltage offset, the cost function is calculated by adding the third term to the cost function of Equation (17) as follows:

$$g_j = \left|F_e^{ref} - \hat{F}_e(k+2)_j\right| + k_\lambda \left\|\lambda_s^{ref}\right| - \left|\hat{\lambda}_s(k+2)_j\right\| + k_{U_{dc}} \frac{\left|\hat{U}_{dc1}(k+2)_j - \hat{U}_{dc2}(k+2)_j\right|}{U_{dc}} \quad j \in \{1,2,3,4\} \quad (22)$$

where U_{dc} is the DC-link voltage which can be calculated by $U_{dc}=U_{dc1}+U_{dc2}$ and k_{Udc} is the weight coefficient of the DC-link capacitor voltage offset reduction.

The proposed method can be implemented as shown is Figure 5. The k, k+1, and k+2 subscripts show the value of variables at k, k+1, and k+2 sampling times respectively. $\vec{u}_{opt}^{k}$ and $\vec{u}_{opt}^{k+1}$ are the optimal voltage vectors at current repetition loops.

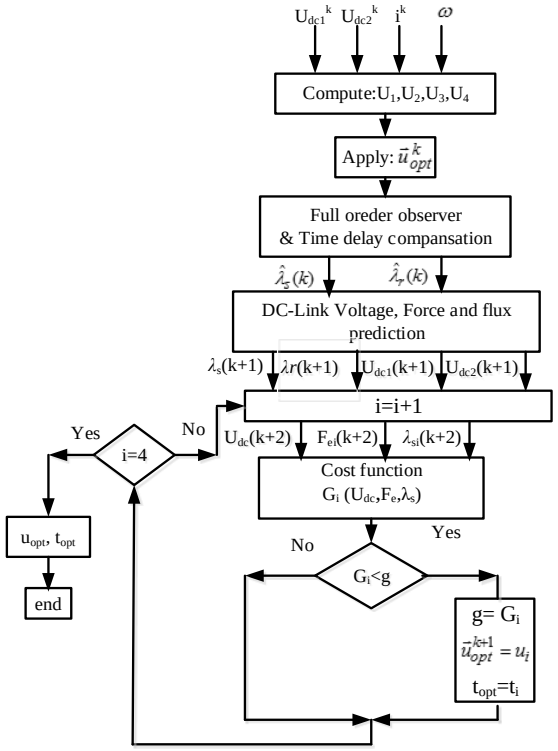

Figure 5. Flowchart of proposed PFC scheme

As mentioned before, a high degree of flexibility is optained by the proposed control method due to its online optimization algorithm, The uncertainties and limitations of the system (i.e. the capacitor voltage offset) could be considered in the cost function.

4. ANALLYSIS AND DISCUSSION OF THE WEIGHT COEFFICIENT

According to Equation (22), it is clear that only the weight coefficients are adjustabls in the cost function in the proposed method. Therefore, it is essential to analyze and discuss the effects of such parameters. However, no method has been introduced for calculation of the values of these parameters. Thereupon, such values are calculated by the simulation. In order to analyze the effects of weight coefficients, simulations have been performed for several different LIMs in MATLAB software and is presented in Table 2. According to this table, the weight coefficients of stator flux and the capacitor voltage offset reduction are calculated from the following relationships:

$$k_{Udc} = \frac{U_{dc} \cdot C}{N_s \cdot T_{dead} \cdot f} \quad (23)$$

TABLE 2. LIMs and inverter specification of with weight coefficient found by simulations

Parameter	Values	k_{Udc}	k_λ	Values	k_{Udc}	k_λ	Values	k_{Udc}	k_λ
LIM									
P_n	2.8 kW			4.8 kW			2.2 kW		
V_n	380 V			380 V			380 V		
V_l	4 m/s			5 m/s			5 m/s		
I_n	2.8 A			3.8 A			4 A		
P	4			6			4		
L_{ls}	86 mH			49 mH			10.33 mH		
L_{lr}	≈ 0 mH			≈ 0 mH			≈ 0 mH		
L_m	100 mH	700	10	150 mH	500	7	100.3 mH	850	9
R_s	3.5 Ω			4.1 Ω			2.8 Ω		
R_r	20 Ω			25 Ω			12 Ω		
M	10 kg			12 kg			10 kg		
Inverter									
U	540 V			460 V			540 V		
C_1	1000 μF			860 μF			1200 μF		
C_2	1000 μF			860 μF			1200 μF		
T_{dead}	4 μs			6 μs			4 μs		
LIM									
P_n	9 kW			8 kW			5 kW		
V_n	380 V			380 V			380 V		
V_l	9 m/s			8 m/s			4 m/s		
I_n	5.5 A			5.2 A			2.8 A		
P	4			4			6		
L_{ls}	74 mH			69 mH			86 mH		
L_{lr}	≈ 0 mH			≈ 0 mH			≈ 0 mH		
L_m	200 mH	2750	1	100 mH	1150	1.5	100 mH	950	0.5
R_s	5.6 Ω			4.6 Ω			4.3 Ω		
R_r	9 Ω			8 Ω			30 Ω		
M	20 kg			20 kg			15 kg		
Inverter									
U	460 V			440 V			480 V		
C_1	4700 μF			2000 μF			1500 μF		
C_2	4700 μF			2000 μF			1500 μF		
T_{dead}	4 μs			4 μs			4 μs		

$$k_\lambda = \frac{N_s \cdot f}{T_{rated} \cdot i_{rated}} \quad (24)$$

4. 1. Weight Cofficient of the Stator Flux The parameters of the simulation and test system studied are provided in Table 3. k_λ is the weight coefficient that increases or decreases the relative importance of force control compared to the flux control. If the importance of both is the same, this coefficient will be equal to 1. Since the currents directly control the stator flux, to establishe balance of the currents in B4 inverter, higher weigh coefficient is expected. According to the Equation (24) and the values given in Table 3, the stator flux weight coefficient is obtained as follows:

$$k_{Udc} = \frac{U_{dc} \cdot C}{N_s \cdot T_{dead} \cdot f} = \frac{540 \cdot \left(2040 \times 10^{-6}\right)}{4 \cdot \left(5.5 \times 10^{-6}\right) \cdot 50} = 1001.45 \approx 1000$$

Figure 6 presents the simulation results using the conventional [20] and proposed methods at the constant speed of 2 m/s and load force of 50 N for the k_λ =3 where

the reference of the stator flux is considered to be 0.9 Wb. As observed in Figure 6, although the higher designation of weight coefficient of stator flux somewhat optimizes the balance of current, because the weight coefficient of the DC-link capacitor voltage offset reduction is ignored, the electromagnetic force has high ripple which causes a unbalance in the waveform of phase current.

4. 2. Weghit Cofficient of the Capacitor Voltage Offset Reduction The k_{Udc} weight coefficient expresses the relative importance of the capacitor voltage offset compared to the control system. With a larger weight coefficient, the voltages of two capacitors converge faster. According to Equation (23) and using the values given in Table 3, the stator flux weight coefficient is obtained as follows:

$$k_{\lambda} = \frac{N_s \cdot f}{T_{rated} \cdot i_{rated}} = \frac{4 \cdot 50}{14 \cdot 4.8} = 2.976 \approx 3$$

In order to analyze the effect of $k_{Udc}$and to prove the value of the weight coefficient obtained by Equation (23), the results are investigated for two values of weight coefficient. The simulation results at the speed of 2 m/s with the nominal force of 50 N.m for k_{Udc}=1000 and k_{Udc}=2000 are shown and analyzed in Figure 7(a), (b), (c), (d). In these figures, behavior of the speed, the electromagnetic force, stator flux, and phase current during of the voltage offset reduction are illustrated. Comparison between Figures 7 for k_{Udc}=1000 and k_{Udc}=2000 and Figure 6 shows that using the weight coefficient and the voltage offset reduction, the force ripple decreases and the motor speed coincides more accurately.

TABLE 3. LIM and inverter pararmeters

Parameter	Values
LIM	
Rated power (P_n)	8.5 kW
Rated voltage (V_n)	290 V
Rated speed (V_l)	5 m/s
Rated current (I_n)	4.8 A
Pole pairs (P)	3
Primary leakage inductance (L_{ls})	69 mH
Magnetizing resistance (L_m)	200 mH
Primary resistance (R_s)	10.6 Ω
Secondary resistance (R_r)	30 Ω
Moving mass (M)	20 kg
Inverter	
DC-link voltage (U)	460 V
DC-link capacitors (C_1, C_2)	860 μF

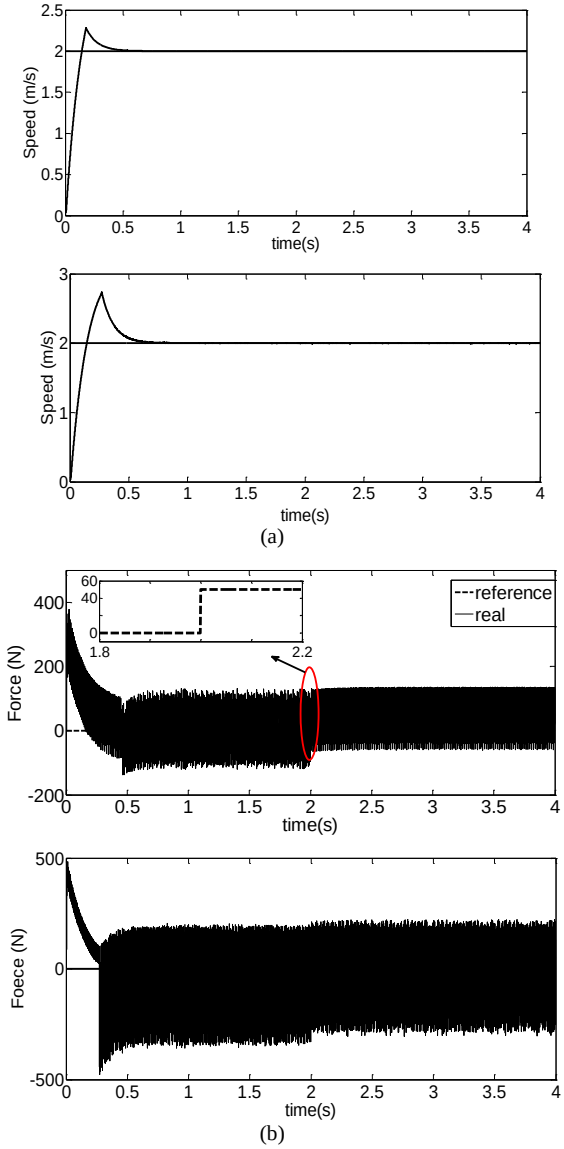

Figure 6. (a) Speed (top): proposed method, (bottom): conventional, (b) electromagnetic force (top): proposed method, (bottom): conventional, at constant speed of 2 m/s and load force of 50 N for the k_{λ} =3

Moreover, based on comparison between Figure 7 for k_{Udc}=1000 and k_{Udc}=2000, with proper determination of the weighting coefficient according to Equations (23) and (24), ripple of the stator flux and electromagnetic force decreases. Therefore, a satisfactory performance at k_{Udc}=1000 is achieved.

Simulation results for conventional [20] and proposed methods at the step speed of 2-4 m/s for k_{Udc}=1000 are depicted in Figure 8. Due to the designation of a proper value for the weight coefficient of the capacitor voltage offset reduction in proposed method, the balance of the current improved the ripple of the stator flux, and the ripple of the electromagnetic force is acceptable.

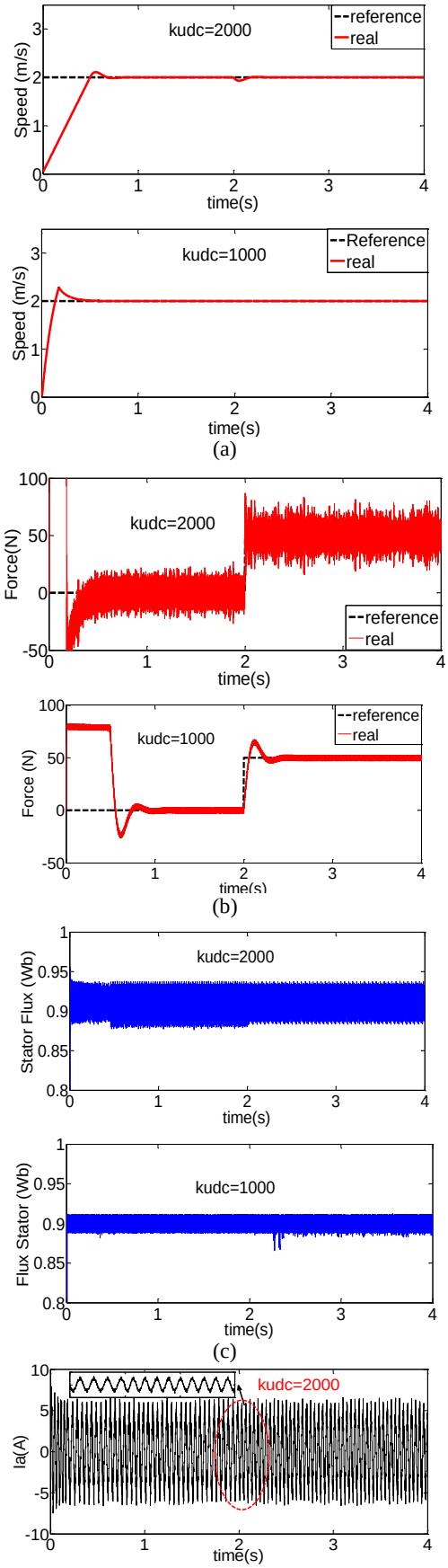

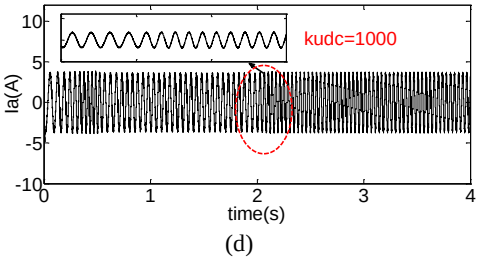

(d)

Figure 7. (a) Speed, (b) force, (c) flux stator, (d) Current of phase "a" at speed of 2 m/s and load force of 50 N for k_{Udc}=2000 and k_{Udc}=1000

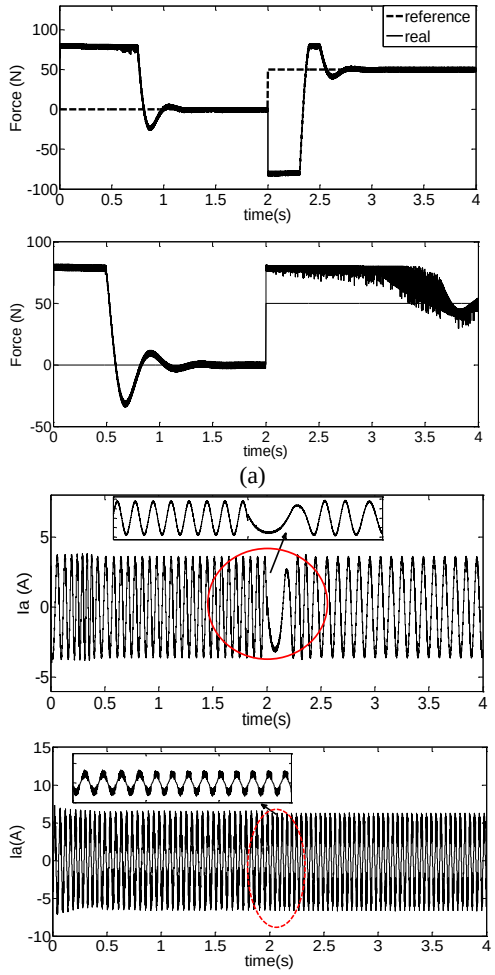

(b)

Figure 8. (a) Electromagnetic force (top): proposed method, (bottom): conventional, (b) Current a-phase (top): proposed method, (bottom): conventional, at speed reference as a step function from 2-4 m/s with load force of 50 N for k_{Udc}=1000

5. CONCLUDING REMARKS

The SMPFC of a LIM with a three-phase 4-switch inverter is analyzed. In order to decrease the ripple of stator flux and electromagnetic force, tuning of weight

coefficient of flux at PFC is employed. Next, to improve performance of the proposed method, a weight coefficient is defined for the capacitor voltage offset reduction, because the balance of currents is inappropriate. In order to analyze the effects of weight coefficients, simulations have been performed for several different LIMs in MATLAB software and the weight coefficients of stator flux and the capacitor voltage offset reduction are calculated from relationships. According to the results of numerical simulations, the balance of the currents is improved by determining the appropriate value for the weight coefficient of the capacitor voltage offset reduction. Furthermore, ripple of the stator flux and electromagnetic force more decreases by determining the appropriate value for the weight coefficient of the capacitor voltage offset reduction compared to the mode where the weight coefficient is only designated for the stator flux.

6. REFERENCES

1. Boldea, I. and Nasar, S.A., "Linear electric actuators and generators", ***IEEE International Conference in Electric Machines and Drives Record***, (1997), MA1/1.1-MA1/1.5.
2. Boldea, I., "Linear electric machines, drives, and maglevs handbook, CRC Press, (2013).
3. Q. F. Lu and W. H. Mei, "Recent development of linear machine topologies and applications," ***CES Transactions on Electrical Machines and Systems***, Vol. 2, No. 1, (2018), 65-72.
4. G. Lv, Z. Liu and S. Sun, "Analysis of Torques in Single-Side Linear Induction Motor With Transverse Asymmetry for Linear Metro," ***IEEE Transactions on Energy Conversion***, Vol. 31, No. 1, (2016), 165-173.
5. D. Campos-Delgado, D. Espinoza-Trejo, and E. Palacios, "Fault-tolerant control in variable speed drives: A survey," ***Electric Power Application., IET***, Vol. 2, No. 2, (2008), 121–134.
6. Francesco Alonge, Maurizio Cirrincione, Marcello Pucci, Antonino Sferlazza, "Input–output feedback linearizing control of linear induction motor taking into consideration the end-effects. Part I: Theoretical analysis", ***Control Engineering Practice,*** Vol 36, (2015), 133-141.
7. B. A. Welchko, T. A. Lipo, T. M. Jahns, and S. E. Schulz, "Fault tolerant three-phase AC motor drive topologies: A comparison of features, cost, and limitations," ***IEEE Transactions on Power Electronics***, Vol. 19, No. 4, (2004), 1108– 1116.
8. F. Blaabjerg, D. O. Neacsu, and J. K. Pedersen, "Adaptive SVM to compensate DC-Link voltage ripple for four-switch three-phase voltage-source inverters," ***IEEE Transactions on Power Electronics***, Vol. 14, No. 4, (1999), 743–752,
9. D. M. Lee, J. B. Park, and H. A. Toliyat, "A simple current ripple reduction method for B4 inverters," ***Journal of Electrical Engineering Technology***, Vol. 8, No. 5, (2013), 1062– 1069
10. R. Wang, J. Zhao, and Y. Liu, "A comprehensive investigation of four-switch three-phase voltage source inverter based on double Fourier integral analysis," ***IEEE Transactions on Power Electronics***, Vol. 26, No. 10, (2011), 2774–2787
11. M. N. Uddin, T. S. Radwan, and M. A. Rahman, "Fuzzy-logic controller- based cost-effective four-switch three-phase inverter-fed IPM synchronous motor drive system," ***IEEE Transactions on Industrial Application***, Vol. 42, No. 1, (2006), 21–30,
12. B. El Badsi, B. Bouzidi, and A. Masmoudi, "DTC scheme for a four-switch inverter-fed induction motor emulating the six-switch inverter operation," ***IEEE Transactions on Power Electronics***, Vol. 28, No. 7, (2013), 3528–3538
13. M. H. Holakooie, M. B. Bannae Sharifian, M.R. Feyzi. "Sensorless indirect field oriented control of single sided linear induction motor with a novel sliding mode MRAS speed estimator," ***International Journal of Engineering (IJE) Transactions A: Basics***, Vol. 28, No. 7, (2015), 1011-1020.
14. Mohammad Hosein Holakooie, Mansour Ojaghi, Asghar Taheri, "Full-order Luenberger observer based on fuzzy-logic control for sensorless field-oriented control of a single-sided linear induction motor", ***ISA Transactions***, Vol. 60, (2016), 96-108.
15. J. H. Lee, "Model predictive control: Review of the three decades of development," ***International Journal of Control, Automation and Systems***, Vol. 9, No. 3, (2011), 415–424.
16. Wenxiang Song, Shengkang Le, Xiaoxin Wu, and Yi Ruan, "An Improved Model Predictive Direct Torque Control for Induction Machine Drives," ***Journal of Power Electronics***, Vol. 17, No. 3, (2017), 674-685.
17. Yasser Shoukry, M. Watheq El-Kharashi, Sherif Hammad, "An embedded implementation of the generalized predictive control algorithm applied to automotive active suspension system," ***Computers & Electrical Engineering***, Vol. 39, No. 2, (2013), 512–529.
18. Fengxiang Wang,Xuezhu Mei,Jose Rodriguez, "Model Predictive Control of Electrical Drive systems- on overview," ***CES Transactions on Electrical Machines and Systems***, Vol. 1, No. 3, (2017), 219-230.
19. S. Kouro, P. Cort´es, R. Vargas, U. Ammann, and J. Rodr´ıguez, "Model predictive control—A simple and powerful method to control power converters," ***IEEE Transactions on Power Electronics***, Vol. 56, No. 6, (2009), 1826–1838.
20. C. A. Rojas, J. Rodriguez, F. Villarroel, J. R. Espinoza, C. A. Silva, and M. Trincado, "Predictive torque and flux control without weighting factors," ***IEEE Transactions on Power Electronics***, Vol. 60, No. 2, (2013), 681–690.
21. G. Kang and K. Nam, "Field-oriented control scheme for linear induction motor with the end effect," ***IEE Proceedings-Electric Power Applications***, Vol. 152, No. 6, (, 2005), 1565–1572.
22. Y. Cho, Y. Bak and K. B. Lee, "Torque-Ripple Reduction and Fast Torque Response Strategy for Predictive Torque Control of Induction Motors," ***IEEE Transavtions on Power Electronics***, Vol. 33, No. 3, (2018), 2458-2470.
23. J. Rodriguez, R. M. Kennel, J. R. Espinoza, M. Trincado, C. A. Silva, and C. A. Rojas, "High-performance control strategies for electrical drives: An experimental assessment," ***IEEE Transactions on Industrial Electronics***, Vol. 59, No. 2, (2012), 812–820.
24. T. Geyer, "Computationally efficient model predictive direct torque control," ***IEEE Transactions on Power Electronics***, Vol. 26, No. 10, (2011), 2804–2816.
25. S. A. Davari, D. A. Khaburi, and R. Kennel, "An improved FCS–MPC algorithm for an induction motor with an imposed optimized weighting factor," ***IEEE Transactions on Power Electronics***, Vol. 27, No. 3, (2012), 1540–1551.
26. Gayathri, M.N., Himavathi, S. and Sankaran, R., "Comparison of mras based rotor resistance estimator using reactive power and flux based techniques for space vector pwm inverter fed induction motor drives", ***International Journal of Engineering-Transaction C: Aspects***, Vol. 25, No. 3, (2012), 205-212.
27. H. Miranda, P. Cortes, J. Yuz, and J. Rodriguez, "Predictive torque control of induction machines based on state-space

models," ***IEEE Transactions on Industrial Electronics***, Vol. 56, No. 6, (2009), 1916 –1924.

28. Fateh, M. and Sadeghijaleh, M., "Voltage control strategy for direct-drive robots driven by permanent magnet synchronous motors", ***International Journal of Engineering-Transactions B: Applications***, Vol. 28, No. 5, (2014), 709-716.

Sensorless Model Predictive Force Control with a Novel Weight Coefficients for 3-Phase 4-Switch Inverter Fed Linear Induction Motor Drives

S. Masomi Kazraji, M. R. Feyzi, M. B. B. Sharifian, S. Tohidi

Faculty of Electrical and Computer Engineering University of Tabriz, Tabriz, Iran

P A P E R I N F O

Paper history:
Received 27 December 2017
Received in revised form 14 April 2018
Accepted 26 April 2018

Keywords:
Linear Induction Motor
Sensorless Model Predictive Force Control
4-switch Inverter
Weight Coefficient

چکیده

کنترل بدون حسگر پیش بین نیرو مبتنی بر مدل (SMPFC) روشی قدرتمندی برای کنترل درایوهای موتور القایی خطی با اینورتر سه فاز ٤ (٦) سوئیچه می‌باشد. این نوع اینورتر می‌تواند برای کنترل تحمل خطا به منظور حل مشکل مدار باز/ اتصال کوتاه در اینورترهای ٦ سوئیچه (B6) به‌کار گرفته شود. این مقاله یک روش برای SMPFC موتور القایی خطی (LIM) تغذیه شده توسط یک اینورتر ٤ سوئیچه به‌همراه کاهش آفست ولتاژ خازن لینک DC پیشنهاد می‌دهد. شبیه‌سازی روی چندین موتور القایی خطی مختلف در نرم‌افزار MATLAB برای تعیین ضرایب وزنی شار استاتور و کاهش آفست ولتاژ خازن انجام شده است. سپس، یک رابطه برای تعیین ضرایب DC در تابع هزینه SMPFC پیشنهاد شده است. با استفاده از روابط ضرایب وزنی در تابع هزینه، بردارهای ولتاژ اینورتر ٤ سوئیچه برای پیش‌بینی دقیق به‌دست آمده است. تعادل بین جریان‌ها با تعیین مقدار مناسب برای ضریب وزنی کاهش آفست ولتاژ خازن بهبود می‌یابد. نتایج شبیه‌سازی برای تأیید روش کنترلی پیشنهادی ارائه شده است.

***doi**: 10.5829/ije.2018.31.09c.09*